Desalination and Water Treatment
www.deswater.com

18 (2010) 182–186
June

1944-3994 / 1944-3986
doi: 10.5004/dwt.2010.1768

Influence of an inhomogeneous membrane charge density on the rejection of electrolytes by nanofiltration membranes

Haochen Zhu[a,b], Anthony Szymczyk[a,b,*], Béatrice Balannec[a,b]

[a]*Université Européenne de Bretagne, France*
[b]*Sciences Chimiques de Rennes, UMR 6226 CNRS - Université de Rennes 1 - ENSCR,*
Campus de Beaulieu, av. du Général Leclerc, 35700 Rennes, France
Tel.: +33 (2) 23 23 65 28; Fax: +33 (2) 23 23 57 65; email: anthony.szymczyk@univ-rennes1.fr

Received 1 June 2009; Accepted 21 December 2009

ABSTRACT

The salt rejection of membranes with inhomogeneous fixed charge densities including both symmetric and asymmetric distributions has been investigated theoretically. The rejection rates for the different fixed charge distributions, have been calculated by using a standard nanofiltration (NF) model based on the extended Nernst-Planck equation, the local electroneutrality condition and a modified Donnan equation including both steric and electrostatic effects and have been compared with the rejection rate obtained for a homogeneous distribution with the same average fixed charge concentration. The effects of the ion diffusion coefficients and the pore radius on the membrane rejection have also been investigated for the various fixed charge distributions. It has been shown that inhomogeneous fixed charge distributions may significantly affect the rejection properties of NF membranes. The value of the fixed charge concentration at the pore inlet plays a major role and high charge densities at the pore inlet tend to increase the salt rejection. Nonetheless, it has also been shown that strong axial gradients of the fixed charge concentration can affect significantly the ion transport within pores.

Keywords: Inhomogeneous fixed charge distribution; Nanofiltration; Rejection rate

---

1. Introduction

The recent extensive development of nanofiltration (NF) technology has put in evidence the real application potentialities in several areas, e.g., textile industry (removal of dye from waste rinse water), paper and plating industries (limitation of the consumption of clean water by recycling waste water), drinking water production, etc.

NF membranes are made of organic or ceramic materials the most of which develop a surface electric charge when immersed in aqueous electrolyte solutions. Since almost all current models [1–6] assume that the fixed charge distribution in the membrane is homogeneous (i.e., the membrane volume charge density is assumed to be independent of the axial position inside pores), the question of how inhomogeneous distributions affect the transport and selectivity of NF membranes naturally arises [7–11]. This problem has been discussed recently in the context of ion exchange membranes [12–19] as well as in some biological ion channels [20–23], but the issue of how inhomogeneous fixed charge distributions act on the rejection of electrolytes by NF membranes has not been addressed yet. Here, we have dropped the assumption of homogeneous

---

*Corresponding author.

fixed charge distributions in order to investigate the influence of spatially asymmetric fixed charge distributions on ions transport through NF membrane. A comprehensive set of 1D distributions have been considered and analyzed on the basis of the Nernst-Planck equations coupled with a local electroneutrality condition. In this work, we have computed the rejection rates of uni-univalent electrolytes by NF membranes with different fixed charge distributions including hyperbolic, linear, skin and cluster distributions (see below). For the sake of clarity, dielectric effects have not been included in calculations. The results have been compared with those obtained with a homogeneously charged membrane with the same average fixed charge concentration. In particular, we have discussed if the occurrence of spatial inhomogeneities in the fixed charge can lead to an enhancement of the rejection rate with respect to the homogeneously charged membranes.

2. Theoretical background

2.1. Extended Nernst-Planck equation

The extended Nernst-Planck equation Eq. (1) describes the solute transport through charged porous membranes and can be written as,

$$j_i = -D_{i,\infty}\frac{dc_i}{dx} - \frac{z_i c_i D_{i,\infty}}{RT}F\frac{d\psi}{dx} + K_{ic}c_iV \tag{1}$$

here $j_{i,}$ and V are represented as Eqs. (2) and (3),

$$j_i = \frac{J_v c_i(\Delta x^+)}{A_k} \tag{2}$$

$$V = \frac{J_v}{A_k} \tag{3}$$

where the value Δx^+ of the axial coordinate means just outside the pore outlet (i.e., in the permeate) (see the List of symbols section for definition of the various symbols).

The extended Nernst-Planck equation describes ion transport in terms of diffusion under the action of the solute concentration gradient, migration under the action of the spontaneously arising electric field and convection due to the solvent flow.

The concentration gradient inside pores can be obtained by rearranging Eq. (1),

$$\frac{dc_i}{dx} = -\frac{J_v c_i(\Delta x^+)}{D_{i,\infty}A_k} - \frac{z_i c_i}{RT}F\frac{d\psi}{dx} + \frac{J_v c_i K_{ic}}{D_{i,\infty}A_k} \tag{4}$$

The local electroneutrality condition inside pores reads as follows,

$$\sum_i z_i c_i + X_{loc} = 0 \tag{5}$$

Combining Eqs. (4) and (5), we can establish the expression of the potential gradient inside pores as Eq. (6),

$$\frac{d\psi}{dx} = \frac{\sum_i \frac{J_v z_i}{D_{i,\infty}A_k}\left[c_iK_{ic} - c_i(\Delta x^+)\right] + \frac{dX_{loc}}{dx}}{\frac{F}{RT}\sum_i c_i z_i^2} \tag{6}$$

The distribution of ions at the membrane/solution interfaces is described by the following Donnan equations (Eqs. (7) and (8)) including both the steric hindrance and the Donnan exclusion,

$$\frac{c_i(0^+)}{c_i(0^-)} = \phi_i \exp(-z_i\Delta\psi_{(0^+|\ 0^-)}) \tag{7}$$

$$\frac{c_i(\Delta x^-)}{c_i(\Delta x^+)} = \phi_i \exp(-z_i\Delta\psi_{(\Delta x^-|\Delta x^+)}) \tag{8}$$

where the values of the axial coordinate 0^- and 0^+ denote the position just outside and just inside the pore inlet, respectively, and Δx^- and Δx^+ denote the position just inside and just outside the pore outlet, respectively. $0^+ | 0^-$ and $\Delta x^- | \Delta x^+$ denote the membrane/solution interfaces at the feed side and the permeate side, respectively.

For the sake of clarity, dielectric effects have not been included in the above partitioning equations although dielectric exclusion is likely to affect significantly the rejection properties of NF membranes[24]. Finally, the rejection rate R_i is calculated for a solute i according to its definition by Eq. (9):

$$R_i = 1 - \frac{c_i(\Delta x^+)}{c_i(0^-)} \tag{9}$$

2.2. Different fixed charge distributions

Fig. 1(a–d) shows the four fixed charge distributions under consideration in the present work, the expressions of which are represented by Eqs. (10)–(13),

Hyperbolic

$$X_{loc} = \frac{-10}{(0.0745 + 4\overline{x})} \tag{10}$$

Linear

$$X_{loc} = 20\overline{x} - 20 \tag{11}$$

Skin

$$X_{loc} = -120\overline{x}^2 + 120\overline{x} - 30 \tag{12}$$

Cluster

$$X_{loc} = -10\sin 8\pi\overline{x} - 10 \tag{13}$$

in which $\overline{x} = x/\Delta x$, is the dimensionless axial coordinate (Δx being the membrane thickness).

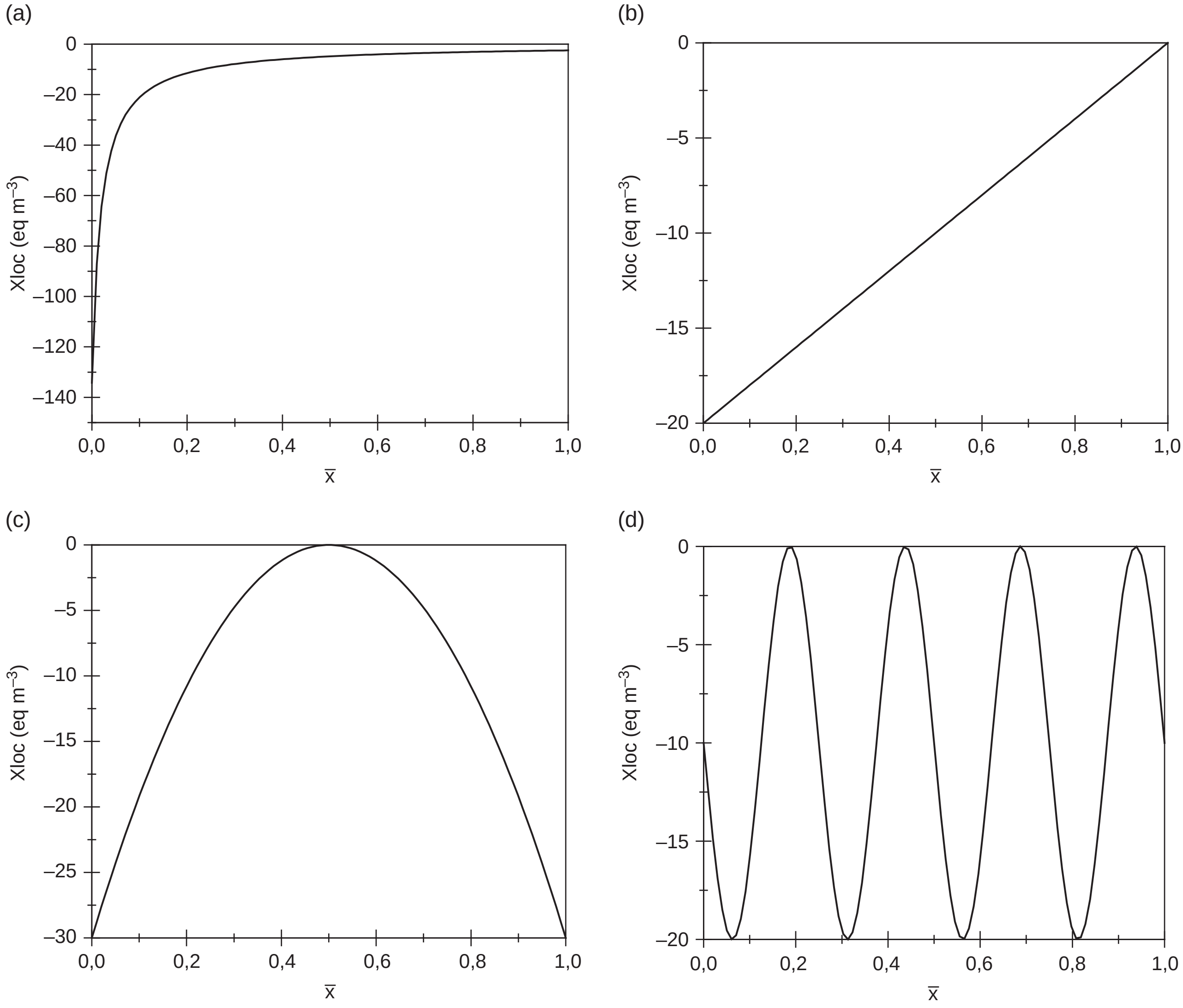

Fig. 1. Inhomogeneous fixed charge distributions under consideration; (a) Hyperbolic; (b) Linear; (c) Skin; (d) Cluster.

The axial profiles correspond to typical symmetric and asymmetric pores and include most of the cases that could be found in practical situations. The skin distribution may result from usual membrane preparation procedures and could also find application in the case of double conical track-etched pores. The cluster distributions are typical of pores where a hydrophobic structure is superimposed to cluster like hydrophilic regions containing the charged groups, the water molecules, and the mobile ions[25].

In order to allow a better comparison between the different distributions, all the distributions presented here have been chosen to give the same average charge concentration ($X_{loc}^{avg} = -10$ eq m^{-3}) over the membrane thickness.

3. Results and discussion

Fig. 2(a–c) shows the variation of the theoretical rejection rate of a millimolar solution of uni-univalent electrolyte with the permeate volume flux for the various fixed charge distributions (homogeneous and inhomogeneous) and various ion diffusion coefficients. It is clearly shown that the inhomogeneous distribution of fixed charges significantly affect the separation performances of the membrane although the average fixed charge concentration is identical for all the charge distributions under consideration and that it is possible to increase the salt rejection by using an appropriate fixed charge distribution. The sequence $R_{\text{Hyperbolic}} > R_{\text{Skin}} > R_{\text{Cluster}}$ indicates the dominant role of pore inlet effects since the rejection rate increases as

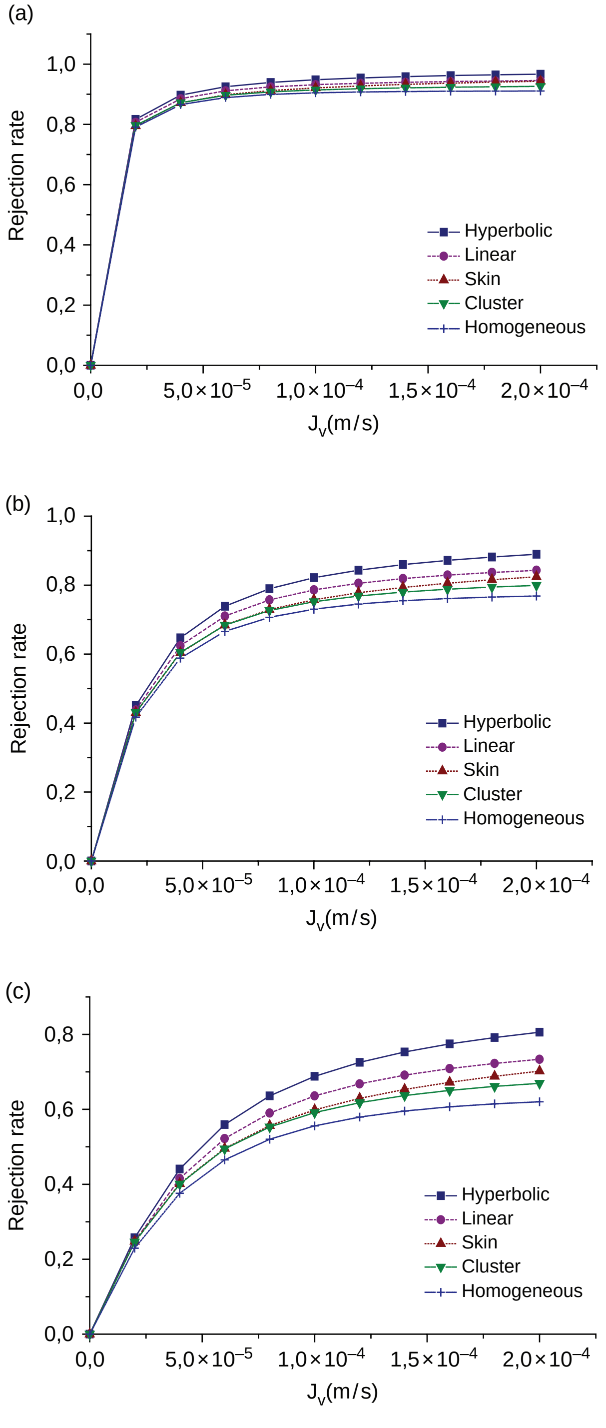

Fig. 2. Rejection rate of a millimolar solution of uni-univalent electrolyte vs. permeate volume flux for the various fixed charge distributions; r_p = 1 nm; $\Delta x/A_k$ = 5 µm; (a) $D_+ = D_- = 10^{-9}$ m/s²; (b) $D_- = 2D_+ = 2 \times 10^{-9}$ m/s²; (c) $D_- = 3D_+ = 3\times 10^{-9}$ m/s².

the charge density at the pore inlet increases in absolute value (the value of X_{loc} at the pore inlet is –134, –30 and –10 eq m^{-3} for the hyperbolic, skin and cluster distributions, respectively).

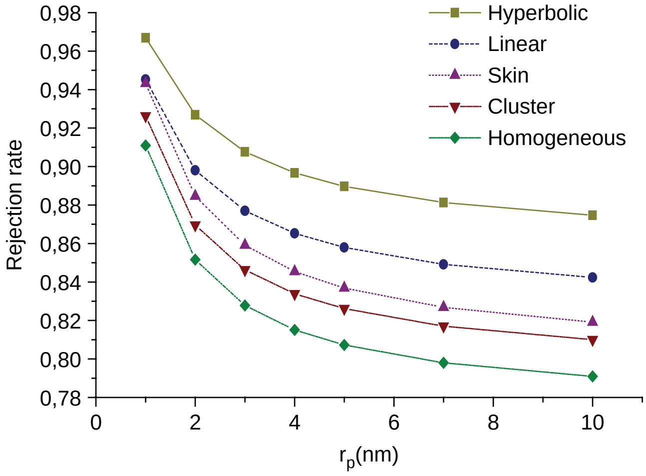

Fig. 3. Variation of the rejection rate vs. the pore radius for the different fixed charge distributions at $J_v = 2 \times 10^{-4}$ m/s; $\Delta x/A_k$ = 5 µm; $D_+ = D_- = 10^{-9}$ m/s².

It can be noted, however, that $R_{\text{Linear}} > R_{\text{Skin}}$ although the fixed charge concentration at the pore inlet is lower for the linear distribution (X_{loc} = –20 eq m^{-3} at the pore inlet). The reason is that the fixed charge decreases much more strongly for the skin distribution than for the linear one. The rejection rate is higher for the cluster distribution than for the homogeneous distribution although the fixed charge concentration at the pore inlet is the same in both cases because the fixed charge density of the cluster distribution increases (in absolute value) just after the pore inlet.

As expected, Fig. 2(a–c) shows that the increase in the coion diffusivity decreases the rejection rate of electrolytes but it can be noted that the variation in the ion diffusion coefficient does not modify the sequence of rejection rates obtained with the various fixed charge distributions.

Figure 3 shows the variation of the rejection rate versus the membrane pore radius for different fixed charge distributions. As expected, the rejection rate decreases as the pore size increases due to the weaker steric hindrance but the effect of the various charge distributions on the rejection rate remains identical (qualitatively) to the one obtained in Fig. 2(a–c).

4. Conclusion

A standard NF model based on the extended Nernst-Planck equation, the local electroneutrality condition and a modified Donnan equation including both steric and electrostatic effects has been used to calculate the theoretical rejection rate of nanoporous membranes with different fixed charge distributions. The results have been compared with those obtained for the case of a homogeneously charged membrane.

It is clearly shown that the inhomogeneous distribution of fixed charges significantly affect the separation performances of the membrane although the average fixed charge concentration is identical for all the charge distributions.

Nomenclature

A_k	porosity of the membrane active layer
c_i	concentration of ion *i*
$D_{i,\infty}$	bulk diffusion coefficient of ion i at infinite dilution
F	Faraday constant
j_i	molar flux density of ion *i*
J_v	permeate volume flux
$K_{i,c}$	hydrodynamic coefficient accounting for the effect of pore walls on convective transport
r_p	pore radius
R	ideal gas constant
R_i	rejection rate of ion *i*
T	temperature
V	solvent velocity inside pores
x	axial coordinate
Δx	effective thickness of the active layer
$\bar{x}$	dimensionless axial coordinate
X_{loc}	local fixed charge concentration
z_i	charge number of ion *i*

Greek symbols

φ	steric partitioning coefficient for ion i
ψ	local electrical potential inside pore
$\Delta\psi$	dimensionless Donnan potential

References

[1] W.R. Bowen, A.W. Mohammad and N. Hilal, Characterisation of nanofiltration membranes for predictive purposes—use of salts, uncharged solutes and atomic force microscopy, J. Memb. Sci., 126 (1997) 91–105.

[2] X.-L. Wang, T. Tsuru, S.-i. Nakao and S. Kimura, The electrostatic and steric-hindrance model for the transport of charged solutes through nanofiltration membranes, J. Memb. Sci., 135 (1997) 19–32.

[3] J. Palmeri, P. Blanc, A. Larbot and P. David, Theory of pressure-driven transport of neutral solutes and ions in porous ceramic nanofiltration membranes, J. Memb. Sci., 160 (1999) 141–170.

[4] C. Labbez, P. Fievet, A. Szymczyk, A. Vidonne, A. Foissy and J. Pagetti, Analysis of the salt retention of a titania membrane using the "DSPM" model: Effect of pH, salt concentration and nature, J. Memb. Sci., 208 (2002) 315–329.

[5] X. Lefebvre, J. Palmeri and P. David, Nanofiltration theory: an analytic approach for single salts, J. Phys. Chem. B., 108 (2004) 16811–16824.

[6] D.L. Oatley, B. Cassey, P. Jones and W. Richard Bowen, Modelling the performance of membrane nanofiltration—recovery of a high-value product from a process waste stream, Chem. Eng. Sci., 60 (2005) 1953–1964.

[7] A. Fulinski, I.D. Kosinska and Z. Siwy, On the validity of continuous modelling of ion transport through nanochannels, EPL (Europhys. Lett.), 67 (2004) 683–690.

[8] J. Cervera, B. Schiedt and P. Ramirez, A Poisson/Nernst-Planck model for ionic transport through synthetic conical nanopores, EPL (Europhys. Lett.), 71 (2005) 35–41.

[9] J. Cervera, B. Schiedt, R. Neumann, S. Mafe and P. Ramirez, Ionic conduction, rectification, and selectivity in single conical nanopores, J. Chem. Phys., 124 (2006) 104706–9.

[10] Z. Siwy, I.D. Kosinska, A. Fulinski and C.R. Martin, Asymmetric diffusion through synthetic nanopores, Phys. Rev. Lett., 94 (2005) 048102–4.

[11] I.D. Kosinska, How the asymmetry of internal potential influences the shape of I-V characteristic of nanochannels, J. Chem. Phys., 124 (2006) 244707–7.

[12] C. Selvey and H. Reiss, Ion transport in inhomogeneous ion exchange membranes, J. Memb. Sci., 23 (1985) 11–27.

[13] S.A. Kuehl and R.D. Sanderson, J.Phys.Chem., 92 (1985) 517.

[14] J. Pellicer, J.A. Manzanares and S. Mafe, The mercury-in-glass thermometer of non-uniform capillary tube, Physics Education, 26 (1991) 384–386.

[15] S. Koter, Influence of the layer fixed charge distribution on the performance of an ion-exchange membrane, J. Memb. Sci., 108 (1995) 177–183.

[16] J.-P. Hsu, K.-C. Ting and Y.-H. Shieh, Current efficiency of an ion-exchange membrane: effect of piecewise continuous fixed charge distribution, J. Phys. Chem. B., 104 (2000) 3492–3495.

[17] R. Yamamoto, H. Matsumoto and A. Tanioka, Ionic transport behavior across charged membranes with low water content, I. Theoretical aspect of membrane potentials in membranes having inhomogeneously distributed fixed-charge groups, J. Phys. Chem. B., 107 (2003) 10615–10622.

[18] M. Higa and T. Yamakawa, Design and preparation of a novel temperature-responsive ionic gel. 1. A fast and reversible temperature response in the charge density, J. Phys. Chem. B., 108 (2004) 16703–16707.

[19] E.-Y. Choi, H. Strathmann, J.-M. Park and S.-H. Moon, Characterization of non-uniformly charged ion-exchange membranes prepared by plasma-induced graft polymerization, J. Memb. Sci., 268 (2006) 165–174.

[20] A. Alcaraz, E.M. Nestorovich, M. Aguilella-Arzo, V.M. Aguilella and S.M. Bezrukov, Salting out the ionic selectivity of a wide channel: The asymmetry of OmpF, Biophys. J., 87 (2004) 943–957.

[21] I. Kosztin and K. Schulten, Fluctuation-driven molecular transport through an asymmetric membrane channel, Phys. Rev. Lett., 93 (2004) 238102.

[22] M. Aguilella-Arzo, J. Cervera, P. Ramirez and S. Mafe, Blocking of an ion channel by a highly charged drug: Modeling the effects of applied voltage, electrolyte concentration, and drug concentration, Phys. Rev. E Stat. Nonlin. Soft. Matter Phys., 73 (2006) 041914–6.

[23] A. Alcaraz, P. Ramirez, E. Garcia-Gimenez, M.L. Lopez, A. Andrio and V.M. Aguilella, A pH-tunable nanofluidic diode: electrochemical rectification in a reconstituted single ion channel, J. Phys. Chem. B., 110 (2006) 21205–21209.

[24] A. Szymczyk, N. Fatin-Rouge, P. Fievet, C. Ramseyer and A. Vidonne, Identification of dielectric effects in nanofiltration of metallic salts, J. Memb. Sci., 287 (2007) 102–110.

[25] P. Ramirez, V. Gomez, J. Cervera, B. Schiedt and S. Mafe, Ion transport and selectivity in nanopores with spatially inhomogeneous fixed charge distributions, J. Chem. Phys., 126 (2007) 194703–9.